Monatshefte für Chemie 131, 1253–1265 (2000)

Monatshefte für Chemie
Chemical Monthly

Syntheses and Crystal Structures of Polynuclear Cu(I) Complexes Containing the 1,1′-Bis-(diphenylphosphino)-ferrocene Ligand

Patrícia Pinto[1], **Maria J. Calhorda**[1,2,*], **Vitor Félix**[3,*], **Teresa Avilés**[4], and **Michael G. B. Drew**[5]

[1] ITQB, Apart. 127, P-2781-901 Oeiras, Portugal
[2] Departamento de Química e Bioquímica, Faculdade de Ciências, Universidade de Lisboa, P-1749-016 Lisboa, Portugal
[3] Departamento de Química, Universidade de Aveiro, P-3810-193 Aveiro, Portugal
[4] Departamento de Química, Centro de Química Fina e Biotecnologia, FCT, Universidade Nova de Lisboa, P-2825-114 Caparica, Portugal
[5] Department of Chemistry, University of Reading, Whiteknights, Reading RG6 6AD, UK

Summary. The reaction between $[Cu(NCMe)_4][PF_6]$ and 1,1′-*bis*-(diphenylphosphino)-ferrocene (*dppf*) in several ratios, solvents, and conditions led to the synthesis and structural characterization of the Cu(I) complexes $[Cu(dppf)(Odppf)][PF_6]$ (**1**), $[(dppf)Cu(\mu\text{-}dppf)Cu(dppf)][PF_6]_2$ (**2**), and $[(dppf)Cu(\mu\text{-}Cl)_2Cu(dppf)]$ (**3**). Although **1** and the cation in **2** were known, the first was structurally characterized for the first time, exhibiting a significant asymmetry in the coordination sphere of Cu(I) owing to the presence of oxygen. In **2**, the PF_6^- anion led to an interesting crystal packing with large open channels containing water. Finally, DFT calculations on a model of **3** showed that its HOMO exhibits, besides Fe, a significant Cu and Cl character, which is reflected in its electrochemical properties.

Keywords. Copper; *dppf*; Crystal structures; DFT calculations.

Introduction

The complexes of Cu(I) with 1,1′-*bis*-(diphenylphosphino)-ferrocene (*dppf*) have been extensively studied in recent years leading to species containg one or more copper atoms with *dppf* prevailing as chelate (Scheme 1a) or as a bridging ligand (Scheme 1b) [1].

The role played by Cu(I) dimers in proteins such as hemocyanin (oxygen transport) or cytochrome oxidase (oxygen binding) [2] has made the study of such compounds particularly interesting. In mononuclear complexes, Cu(I) tends to adopt a tetrahedral coordination sphere or, less frequently, a triangular arrangement in accordance with the d^{10} electron count. Although tetraphosphine Cu(I) complexes have been synthesized and structurally characterized [3], the related $[(dppf)_2Cu]^+$

* Corresponding authors

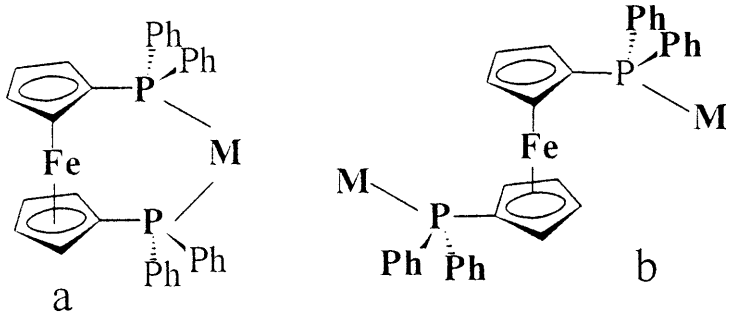

Scheme 1

cation has never been described. Cu(I) cationic complexes are also interesting precursors for the formation of solids using different counterions, leading to new structures and arrangements [4]. On the other hand, organometallic ligands such as *dppf* immediately lead to polynuclear complexes upon coordination and are therefore extremely useful in preparing polymetallic species where the communication between metal centers can be studied and which may exhibit interesting properties [5]. In order to obtain $[(dppf)_2Cu]^+$ and other polynuclear complexes, reactions of $[Cu(NCMe)_4][PF_6]$ with *dppf* were carried out under different conditions. DFT calculations [6] were performed in order to understand the cyclic voltammetry results with respect to the competition between Fe(II) and Cu(I) concerning oxidation.

Results and Discussion

Chemical studies

The reaction between $[Cu(NCMe)_4][PF_6]$ and *dppf* was studied, and different products were isolated depending on the reaction conditions. When the reaction was carried out in ethanol, an orange solid was obtained. Vapor diffusion of ether into a solution of the compound led to the growth of crystals suitable for X-ray diffraction studies. The first batch of crystals was identified as $[Cu(dppf)(OP(Ph)_2C_5H_4FeC_5H_4P(Ph)_2)][PF_6]$ (**1**), $OP(Ph)_2C_5H_4FeC_5H_4P(Ph)_2$ being represented as O*dppf*. **1** is similar to the mixed complex $[Cu(O_2dppf)(dppf)][BF_4]$ where the dioxidized *dppf*, $OP(Ph)_2C_5H_4FeC_5H_4P(Ph)_2O$ (O_2dppf), and *dppf* were used as reagents [1h], and related to the Cu(II) complex $[Cu(O_2dppf)_2][BF_4]_2$ [1d]. In **1**, only one phosphorus atom of *dppf* was oxidized in the course of the reaction, most likely by reaction with the solvent (ethanol) or water (small amounts present in ethanol). This compound has been obtained before, but no structural characterization has been performed [1c]. A second batch of crystals from the same reaction led to the identification of the pentanuclear complex $[(dppf)Cu(\mu\text{-}dppf)Cu(dppf)][PF_6]_2$ (**2**). The perchlorate salt of this cation has been characterized before [7].

In another attempt to prepare $[Cu(dppf)_2]^+$ and to prevent oxidation of the phosphine, the reaction between $[Cu(NCMe)_4][PF_6]$ and *dppf* in a 1:2 ratio was carried out in dry dichloromethane, and crystals were grown by vapor diffusion techniques using dry ether. The crystal structure led to identification of the product

as the new binuclear complex [(*dppf*)Cu(μ-Cl)$_2$Cu(*dppf*)] (**3**). The same product was obtained from several syntheses with different combinations of solvents (always dry) and structurally characterized (see below). The direct reaction between $CuCl_2$ and *dppf* was attempted in order to isolate the Cu(II) analogue of the dimer. Orange crystals were obtained and proven to be **3**.

Solid state structures

The crystal structures of the three Cu(I) complexes [Cu(*dppf*)(OP(Ph)$_2$C$_5$H$_4$-FeC$_5$H$_4$P(Ph)$_2$)][PF$_6$] $\cdot$ 0.5C$_7$H$_8$ (**1**), [(*dppf*)Cu(μ-*dppf*)Cu(*dppf*)][PF$_6$]$_2$ $\cdot$ 0.75H$_2$O (**2**), and [(*dppf*)Cu(μ-Cl)$_2$Cu(*dppf*)] $\cdot$ 0.5CH$_2$Cl$_2$ (**3**) were determined. Complex **1** contains one copper center, whereas both **2** and **3** have two copper centers. Selected bond lengths and angles in the copper coordination sphere of complexes **1**–**3** are given in Table 1.

The crystal structure of **1** contains an asymmetric unit composed by one monomeric [Cu(*dppf*)(O*dppf*)]$^+$ cation and one toluene molecule with an occupation factor of 0.5. A detailed analysis of the structural features of the complex cation is limited by the low quality of X-ray data (see Experimental). However, the structure is determined unequivocally and provides a detailed characterization of the copper coordination sphere.

Table 1. Bond distances (Å) and angles (°) in the Cu(I) coordination spheres of **1**, **2**, and **3**; the prime denotes the symmetry operation $-x + 1/2$, $-y + 3/2$, $-z + 2$

[(*dppf*)Cu(O*dppf*)]$^+$ (**1**)			
Cu-P(1)	2.301(7)	Cu-P(3)	2.299(9)
Cu-P(2)	2.332(8)	Cu-O(1)	2.43(2)
Fe(1)-Cp(1)	1.65(1)	Fe(1)-Cp(2)	1.68(1)
Fe(2)-Cp(3)	1.63(1)	Fe(2)-Cp(4)	1.64(1)
P(1)-Cu-P(2)	106.5(3)	P(3)-Cu-P(1)	116.7(3)
P(3)-Cu-P(2)	125.4(3)	P(3)-Cu-O(1)	103.4(6)
P(1)-Cu-O(1)	93.8(6)	P(2)-Cu-O(1)	105.5(5)
[(*dppf*)Cu(μ-*dppf*)Cu(*dppf*)]$^{2+}$ (**2**)			
Cu-P(1)	2.280(3)	Cu-P(2)	2.283(3)
Cu-P(3)	2.260(3)		
Fe(1)-Cp(1)	1.666(5)	Fe(1)-Cp(2)	1.647(5)
Fe(2)-Cp(3)	1.672(6)		
P(1)-Cu-P(2)	111.3(1)	P(3)-Cu-P(1)	123.4(1)
P(3)-Cu-P(2)	124.6(1)		
[(*dppf*)Cu(μ-Cl)$_2$Cu(*dppf*)] (**3**)			
Cu-P(1)	2.283(2)	Cu-Cl	2.365(2)
Cu-P(2)	2.271(2)	Cu-Cl′	2.434(2)
Fe-Cp(1)	1.648(3)	Fe-Cp(2)	1.643(3)
Cl-Cu-Cl′	95.9(1)	P(1)-Cu-P(2)	111.2(1)
P(1)-Cu-Cl′	99.7(1)	P(1)-Cu-Cl	113.2(1)
P(2)-Cu-Cl	116.2(1)	P(2)-Cu-Cl′	118.8(1)
Cu-Cl-Cu′	84.1(1)		

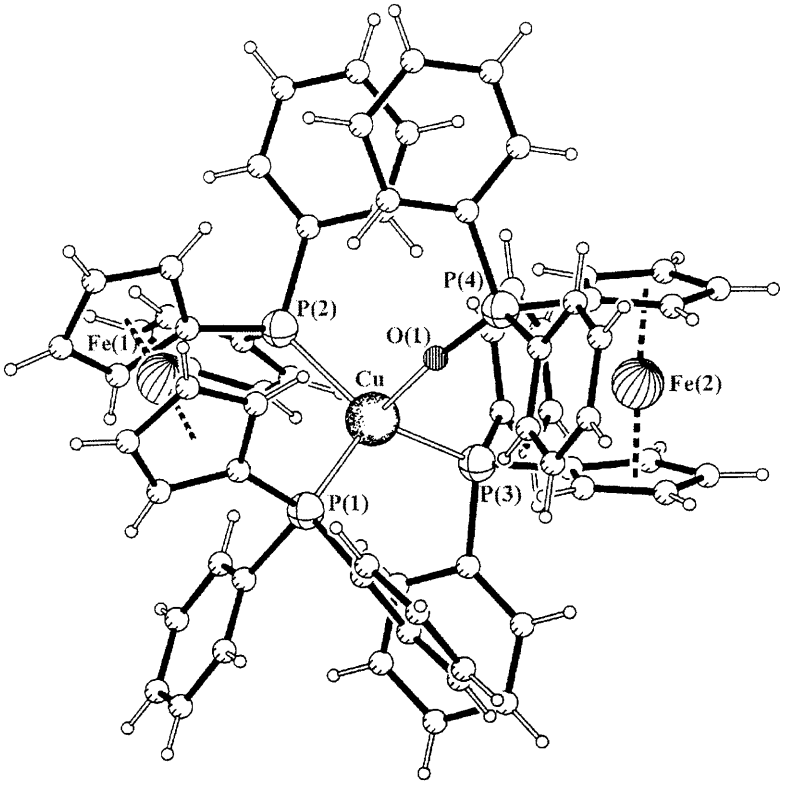

Fig. 1. PLUTON view of [Cu(*dppf*)(O*dppf*)]$^+$ (**1**) showing its overall geometry; for the sake of clarity, only the atom labeling scheme for the atoms quoted in the text is included

In Fig. 1, a molecular diagram of the trinuclear [Cu(*dppf*)(O*dppf*)]$^+$ cation is represented, showing the four-coordinated copper center bound to two phosphorus atoms from a *dppf* ligand and one phosphorus and one oxygen atom from a monooxidized *dppf* ligand (O*dppf*). The crystal structures of two related copper complexes containing two doubly oxidized ligands ([Cu(O_2*dppf*)$_2$]$^{2+}$ (**4**) [1d]) or only one O_2*dppf* moiety ([Cu(O*dppf*)(*dppf*)]$^+$ (**5**) [1h]) have been determined before, although the Cu(II) complex **4** cannot be directly compared. The insertion of one or two oxygen atoms in the Cu(I) coordination sphere has a significant structural effect on the overall geometry of the complexes **1** and **5**. They exhibit a distorted tetrahedral coordination environment with P(1)-Cu-P(2) and O-Cu-P(3) bite angles of 106.5(3) and 103.4(6)° in **1** and P-Cu-P and O-Cu-O angles of 110.1(4) and 102.1(6)° in **5**. In the Cu(II) complex **4** the four oxygen atoms form a distorted square-planar arrangement around the metal center, leading to O-Cu-O bite angles of 154.0(4) and 152.8(4)°. This geometry results from the electronic preferences of the Cu(I) d^9 metal center, in contrast to the preference of Cu(I) d^{10} centers for a tetrahedral coordination. In complex **1** the three Cu-P distances are comparable, falling in the range of 2.299(9)–2.332(8) Å, but the average Cu-P distance of 2.311(8) Å is slightly longer than that reported for complex **5** (2.271(4) Å). On the other hand, the Cu-O distance of 2.43(2) Å in **1** is significantly longer than found for Cu-O distances in **5** (2.111(7) and 2.114(7) Å). In complex **4**,

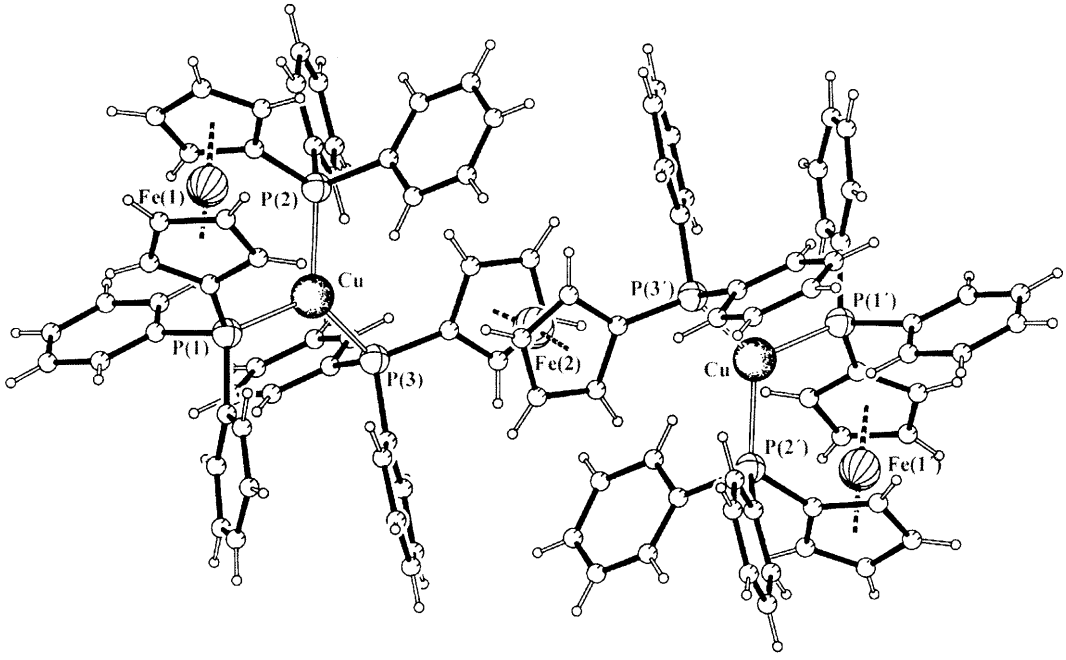

Fig. 2. PLUTON view of [(*dppf*)Cu(*μ-dppf*)Cu(*dppf*)]$^{2+}$ (**2**) showing its overall geometry; for details, see Fig. 1

the shorter Cu-O distances (average value 1.93(1) Å) reflect the higher formal charge on the metal. In complex **1**, the two Cp_2Fe units of O*dppf* and *dppf* exhibit conformations between staggered and eclipsed, but with different values for the α torsion angle of the cyclopentadienyl rings. In this work, α is defined as the angle determined by the centroids of two *Cp* rings and the carbon atoms bound to the phosphorus atom, attaining values of 67.9 and $-22.6°$ for O*dppf* and *dppf* in **1** and -86.6 and 37.2° for O_2*dppf* and *dppf* in **5**.

Figure 2 presents the molecular structure of the pentanuclear cation [(*dppf*)Cu(*μ-dppf*)Cu(*dppf*)]$^{2+}$ (**2**). Two (*dppf*)Cu units are connected by a *dppf* bridge in a centrosymmetric arrangement which is crystallographically imposed. Therefore, the two *Cp* rings in the centre adopt a perfect staggered conformation with a torsional angle of 180.0°. In the terminal *dppf* units, the *Cp* rings display again conformations between a staggered and an eclipsed arrangement with α-values of 37.4°, as found in the tetranuclear systems described above. The angles P-Cu-P of 124.6(1), 123.4(1), and 111.3(1)° found for two copper centres indicate distorted trigonal coordination spheres. The Cu-P distances are within the expected values (see Table 2). The structure of this pentanuclear cation had been determined before as a ClO_4^- salt by X-ray analysis [7] whereas here we show the structure of the PF_6^- salt. It crystallizes in the space group C_2/c; the ClO_4^- salt consists of one asymmetric unit composed of two [(*dppf*)Cu(*μ-dppf*)Cu(*dppf*)]$^{2+}$ cations and four ClO_4^- anions and crystallizes in space group $P\bar{1}$.

Interestingly, the complex cation has very similar structures in both salts. In fact, alignment of the atomic positions of the 113 non-hydrogen atoms of the cations of

Table 2. Molecular dimensions of dimeric Cu(I)*dppf* derivatives containing Cu-*X* bridges α and β are defined in the text; general formula: [(*dppf*)Cu(μ-*X*)$_2$Cu(*dppf*)]

Distances/Å Angles/°	X = Cl^- **3**	X = I^- **6**	X = NO_3^- **7**	X = HCO_2^- **8**
Distances/Å				
Cu...Cu	3.216(2)	3.527	3.429	4.561
Cu...Fe	4.060(1)	4.043	3.967	4.058
⟨Cu-P⟩	2.277(2)	2.283(9)	2.259(6)	2.260(2)
⟨Cu-X⟩	2.400(2)	2.692(6)	2.162(6)	2.083(4)
Angles/°				
Cu-X-Cu	84.1(1)	81.8(2)	104.9(3)	–
X-Cu-X	95.9(1)	98.2(2)	72.6(3)	98.1(2)
P-Cu-P	111.2(1)	111.2(4)	117.8(1)	110.8(1)
X-Cu-P	99.7(1)–118.8(1)	100.5(4)–119.1(3)	100.3(3)–130.3(4)	108.0(1)–121.5(1)
α	42.7	41.8	45.1	37.6
β	83.4(1)	85.9	78.5	85.3
Ref	This work	8	8	8

the two salts leads to root mean square deviations (*rms*) of 0.154 and 0.150 Å. The two independent molecules present in the crystal of the ClO_4^- salt are identical (*rms* = 0.023 Å).

The molecular assembly of PF_6^- anions and [(*dppf*)Cu(μ-*dppf*)Cu(*dppf*)]$^{2+}$ cations results in the formation of large open channels when the crystal packing is viewed along the crystallographic *c* axis as shown in Fig. 3. The diameter of the channels is *ca.* 10.1 Å, which is the average distance between the fluorine atoms sheathing the cavities. These channels accommodate water molecules with occupation factors set to 0.25 and 0.50, respectively (see Experimental). Furthermore, the PF_6^- groups are localized on the surface of the walls, suggesting that the crystal structure is stabilized through hydrogen bonding interactions of the type O–H···F. Unfortunately, the PF_6^- anions are disordered, and the hydrogen atoms of water molecules were not included in the refinement, thus preventing the detailed analysis of these hydrogen bonds. In contrast to the PF_6^- salt, the molecular assembly of [(*dppf*)Cu(μ-*dppf*)Cu(*dppf*)]$^{2+}$ and ClO_4^- results in no specific order in the crystal. Therefore, the replacement of ClO_4^- by PF_6^- has a remarkable effect on the crystal structure channels.

The molecular structure of the tetranuclear complex [(*dppf*)Cu(μ-Cl)$_2$Cu(*dppf*)] (**3**) is shown in Fig. 4. Two (*dppf*)Cu units are linked by two Cl bridges in a centrosymmetric arrangement, the center of the Cu(μ-Cl)$_2$Cu core being localized at a crystallographic inversion center.

A CSD search [3] revealed seven complexes in which two *dppf* transition metal units are connected by two bridging ligands. Three of them are copper complexes: [(*dppf*)Cu(μ-I)$_2$Cu(*dppf*)] (**6**) [8], [(*dppf*)Cu(μ-NO_3)$_2$Cu(*dppf*)] (**7**) [8], and [(*dppf*)Cu(μ_2-HCO_2)$_2$Cu(*dppf*)] (**8**) [8]. Complexes **6** and **7** exhibit the same arrangement as **3**, with two *dppf* Cu units connected *via* two bridges of iodide (**6**) or oxygen from a nitrate ligand (**7**). In complex **8** the two bridges are formed by formate, bridging the metals by two oxygen atoms and thus forming an eight-

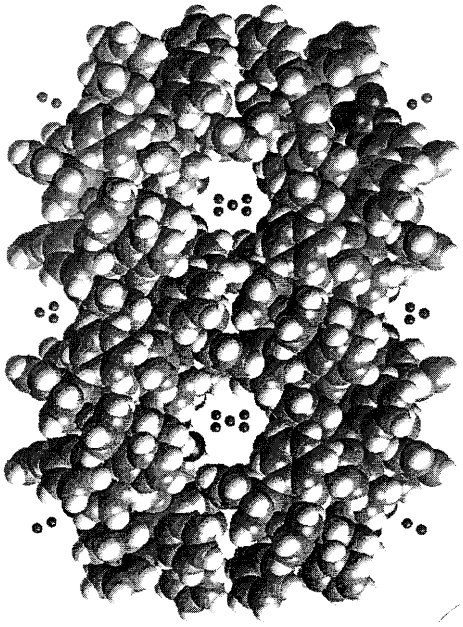

Fig. 3. Crystal packing diagram of [(*dppf*)Cu(μ-*dppf*)Cu(*dppf*)][PF_6]$_2 \cdot 0.75H_2O$ (**2**) view along the crystallographic *c* axis, showing how the assembled cations and anions define the channels which accommodate water molecules

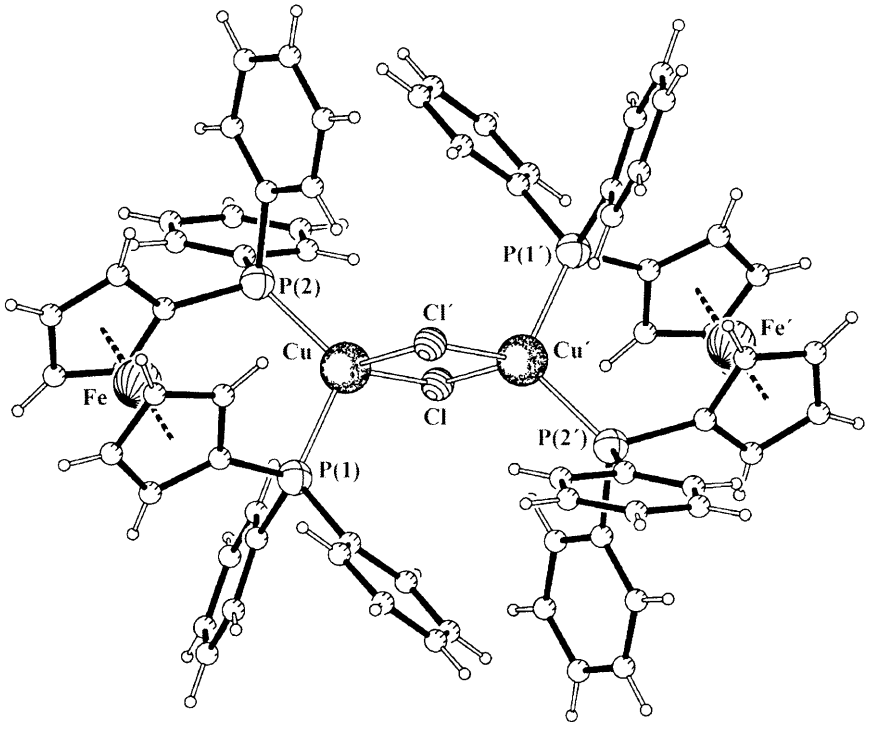

Fig. 4. PLUTON view of [(*dppf*)Cu(μ-Cl)$_2$Cu(*dppf*)] (**3**) showing its overall geometry; for details, see Fig. 1

membered ring. Structural parameters relevant for the characterization of the Cu(I) coordination spheres of these tetranuclear systems and **3** are given in Table 2. All complexes exhibit a distorted tetrahedral coordination. The plane of the bridge, defined in **3** by the two copper centres and the two chlorine atoms, is almost perpendicular to the plane defined by the four phosphorus atoms. The dihedral angle between these two planes (β) is 83.4(1)° for **3**. The Cu···Cu distance of 3.216(2) Å in **3** is much shorter than in **6** (3.527 Å), and it is unexpected when compared with that reported for complex **7** (3.429 Å), since the average Cu-*X* distances are 2.162(6), 2.340(2), and 2.692(6) Å in **7**, **3**, and **6** ($X = O,\ Cl,\ I$). In other words, the Cu···Cu distance in **3** should be situated between the distances reported for **6** and **7**. However, the Cu-Cl-Cu angle in **3** is smaller by *ca.* 21° than the Cu-O-Cu angle in **7**, allowing a closer approach of the two copper centres in the studied complex. As expected, **8** exhibits the longest Cu···Cu distances (4.561 Å), each bridge involving the three-atomic carboxylate group of a formate ligand. Cu(I)···Cu(I) distances as a function of the type of bridge have been discussed in detail in Ref. [9].

The two Cp_2Fe units in the *dppf* ligands exhibit identical conformations between a staggered and an eclipsed arrangement, with torsion angles (α) of 37.6 and 45.1°. Furthermore, the bite angles P-Cu-P and Cu-P distances are comparable in all complexes. In **3** the iron centers are located ±0.465(3) Å above and below of the least squares plane determined by the two copper atoms and two chlorine bridges. Deviations of similar magnitudes were found for the other related complexes (Table 2). This geometric arrangement leads to almost constant intermolecular Fe···Cu distances (*ca.* 4.0 Å) for all complexes. The self-assembling of [(*dppf*)Cu(μ-Cl)$_2$Cu(*dppf*)] molecules affords cavities in the crystal which are occupied by disordered CH_2Cl_2 solvent molecules with occupancy factors of 0.25.

Voltammetric studies

Cyclic voltammetry of solutions of the dicopper complex **3** as well as of the *dppf* ligand for comparison was studied in dry dichloromethane. The cyclic voltammogram of *dppf*, as described in Ref. [1i], exhibits a one-electron process and a second peak assigned to the chemical evolution of the primary oxidation product. The $E_{1/2}$ value for the first process is 0.698 V under the conditions employed (scan rate 0.350 V/s). The anodic peak (0.21 V in Ref. [1i]) is observed at 0.302 V. **2** exhibits a simpler behavior under the some conditions, as only one process is observed at $E_{1/2} = 0.467$ V with $\Delta E = 0.144$ V and $i_a/i_c = 1.19$, in surprising agreement with the value reported in Ref. [1a]. The cyclic voltammetry of **3** has not been studied before to our knowledge; it presents a series of complicated processes. The first oxidation takes place at 0.330 mV (0.538 mV for complex **2**), and no reduction counterpart is easily discernible.

DFT calculations

An interesting question arising from voltammetric studies of *dppf* Cu(I) complexes is whether oxidation takes place preferentially at Cu(I) or Fe(II) in *dppf*. As a matter of fact, ferrocene based ligands have been widely used as probes, owing to the sensivity of the ferrocene oxidation potential to its surroundings. The deviations are

usually assigned as perturbations of the Fe(II)/Fe(III) pair. This aspect was also addressed by *Pilloni et al*. in their electrochemical studies of complex **2** [1c]. In order to clarify this point, DFT calculations [6] (ADF program [10]) were performed on a model of [(*dppf*)Cu(μ-Cl)$_2$Cu(*dppf*)] where the phenyl groups were replaced by hydrogen atoms. Complex **2** was also tried, but it exceeded our possibilities and could not be handled. The geometry of model **3** was fully optimized without symmetry constraints and found to be in good agreement with the X-ray determined structure. Indeed, the root mean square deviation between the DFT optimized structure and the corresponding X-ray fragment was 0.045 Å. The Cu$\cdots$Cu distance was found to be 3.088 Å, slightly shorter than the experimental one (3.216 Å). The two Cu-Cl distances exhibited the same asymmetry as in the structure (2.376 and 2.427 Å compared to 2.365 and 2.434 Å).

The HOMO, which is the most important orbital in understanding the electrochemical behavior, is distributed among the metal atoms. It is localized mainly in the two iron atoms (d_{xy} 4.8%, d_{yz} 10.0%, d_{z^2} 3.2%, $d_{x^2-y^2}$ 3.9%, d_{xy} 8.6%), but also in the two copper atoms (d_{xy} 6.5 d%, d_{z^2} 2.0%, $d_{x^2-y^2}$ 5.9%) as well as in the chlorine bridges (5.4% in each). The other contributions are scattered in very small amounts because of the large total number of atoms. This result suggests that the oxidation proceeds mainly from iron, but there is a participation of copper(I) in this process. The role of the Cl bridges is clear, as they also contribute to the HOMO of the molecule, making it antibonding and facilitating oxidation relative to the pentanuclear species **2** where such an interaction is absent.

Conclusions

The crystal structure of the monocationic complex **1** was determined, and it was found that the presence of the oxygen atom introduces a significant distortion in the coordination sphere of Cu(I). Although the cation present in **2** has been structurally characterized earlier, the presence of a different counterion leads to a totally different crystal structure where channels accommodating water molecules are formed. The dicopper(I) complex **3** was synthesized and also structurally characterized. DFT calculations showed that although the oxidation of the *dppf* derivatives starts at the Fe(II) center, at least in the case of **3** there is a significant contribution from Cu and Cl to the HOMO.

Experimental

Syntheses

Commercially available reagents and all solvents were purchased from standard chemical suppliers. All solvents were used without further purification except acetonitrile (dried over CaH_2), CH_2Cl_2 (dried over CaH_2), and diethyl ether (distilled from sodium/benzophenone ketyl). [Cu(NCMe)$_4$][PF$_6$] [11] and *dppf* [12] were synthesized according to literature procedures. ^{1}H NMR spectra were recorded on Bruker AMX-300 (300 MHz) and Bruker ARX-400 (400 MHz) NMR spectrometers in $CDCl_3$ ($\delta = 7.3$ ppm), and CD_2Cl_2 ($\delta = 5.3$ ppm). Elemental analyses (C, H) were carried out at ITQB; their results agreed with the calculated values within experimental error. The IR spectra were recorded on a Unicam Mattson 7000 FTIR spectrometer (KBr pellets).

[Cu(dppf)(OP(Ph)$_2$C$_5$H$_4$FeC$_5$H$_4$P(Ph)$_2$)][PF$_6$] (**1**)

To 20 cm^3 of a solution of 0.373 g [Cu(NCMe)$_4$][PF$_6$] (1 mmol) in EtOH, an equivalent amount of *dppf* (0.554 g, 1 mmol) dissolved in 20 cm^3 toluene was added. The solution was refluxed for 2 h and filtered; upon cooling, an orange precipitate formed which was isolated, washed with diethyl ether, and dried under vacuum. Crystals of **1** suitable for X-ray studies were grown by vapor diffusion of diethyl ether into a solution of **1** in EtOH. **1** was identified by comparison of its ^{31}P NMR spectrum with that of an authentic sample [1c] and by X-ray crystallography.

[(dppf)Cu(μ-dppf)Cu(dppf)][PF$_6$]$_2 \cdot 0.75\,H_2O$ (**2**)

To 20 cm^3 of a solution of 0.373 g [Cu(NCMe)$_4$][PF$_6$] (1 mmol) in dry EtOH, a solution of *dppf* (1.120 g, 2 mmol) dissolved in 20 cm^3 dry toluene was added. The solution was refluxed for 48 h and filtered; upon cooling, an orange precipitate formed which was isolated, washed with diethyl ether, and dried under vacuum (yield: 75%). Crystals of **2** suitable for X-ray studies were grown by vapor diffusion of petroleum ether into a solution of **2** in CH_2Cl_2. **2** was identified by comparison of its ^{31}P NMR spectrum with that of an authentic sample [1a] and by X-ray crystallography.

[(dppf)Cu(μ-Cl)$_2$Cu(dppf)] (**3**)

To 20 cm^3 of a solution of 0.373 g [Cu(NCMe)$_4$][PF$_6$] (1 mmol) in dry CH_2Cl_2, a solution of *dppf* (1.120 g, 2 mmol) dissolved in 20 cm^3 dry CH_2Cl_2 was added. The solution was stirred for 48 h at room temperature, and the solvent was evaporated under vacuum. The yellow residue was extracted with dry CH_2Cl_2; and addition of dry diethyl ether led to the precipitation of a yellow solid (yield: 40%). Crystals of **3** suitable for X-ray studies were grown by vapor diffusion of dry diethyl ether into a solution of **3** in dry CH_2Cl_2.

^{1}H NMR (400 MHz, δ, $CDCl_2$, 25°C): 7.74-7.35 (m, 40H, C_6H_5), 4.37 (s, 8H, C_5H_4), 4.20 (s, 8H, C_5H_4) ppm; ^{31}P NMR (162 MHz, δ, $CDCl_2$, 25°C): -17.7 (s) ppm.

In a different synthesis, a suspension of 0.17 g (1 mmol) $CuCl_2 \cdot 2H_2O$ in CH_2Cl_2 was treated with a solution of 1.11 g (2 mmol) *dppf* in CH_2Cl_2 and stirred at room temperature. After 1 h, all $CuCl_2 \cdot 2H_2O$ had dissolved, and a yellow precipitate formed which was filtered and washed with petroleum ether. Crystals suitable for X-ray studies were grown by vapor diffusion of petroleum ether into a solution of the compound in CH_2Cl_2. They proved to consist of **3** and not of the desired Cu(II) analogue. In principle, oxidation of *dppf* can lead to reduction of Cu(I), and the ^{31}P NMR spectrum recorded before purification showed peaks assignable to P(O).

Crystallography

Crystal data together with refinement details for complexes **1**, **2**, and **3** are given in Table 3. The X-ray data were collected on a MAR research plate system at Reading University using graphite MoK_α radiation. The crystals were positioned at a distance of 70 mm from the image plate. 95 frames were taken at 2° intervals using a counting time between 2 and 10 min adequate to the crystal under study. Data analysis was performed with the XDS program [13]. Intensities were not corrected for absorption effects.

The systematic absences found for **1** are consistent with the orthorhombic space groups *Pna*2$_1$ or *Pnam*. However, the mean values of $|E^2 - 1|$, calculated with SHELXS86 [14], showed an acentric distribution of the *E* values for 0*kl*, *h*0*l*, and *hk*0 projections and full data. Furthermore, the symmetry of the complex was not consistent with the crystallographic inversion center without a disorder model. The *Pna*2$_1$ group was assumed as correct which was confirmed by the successful structure determination. The structures of **1**, **2**, and **3** were solved by a combination of the direct and *Fourier* differences syntheses followed by least-squares refinement. After all positions of non-hydrogen

Table 3. X-Ray data and structure refinement details for complexes **1–3**

	1	**2**	**3**
Empirical formula	$C_{71.5}H_{60}CuF_6Fe_2OP_5$	$C_{102}H_{90}Cu_2F_{12}Fe_3O_{1.50}P_8$	$C_{69}H_{57}Cl_4Cu_2Fe_2P_4$
M	1379.29	2110.13	1390.61
Crystal system	orthorhombic	monoclinic	monoclinic
Space group	$Pna2_1$	$C2/c$	$C2/c$
a/Å	26.738(33)	33.383(42)	24.856(27)
b/Å	21.450(25)	15.175(18)	13.442(17)
c/Å	11.707(14)	26.050(30)	18.811(23)
β/°	(90.0)	126.42(1)	93.12(1)
V/Å^3	6714.3	10619.1	6275.7
Z	4	4	4
D_c/g · cm^{-3}	1.364	1.320	1.472
μ/mm^{-1}	0.918	0.980	1.435
F(000)	2828	4312	2824
θ Range/°	2.69–24.07	2.64–25.98	2.01–25.98
Index ranges *hkl*	0,−13,−11 to 19,13,11	0,0,−29 to 39,18,17	0,−8,−18 to 29,9,22
Reflections collected	6527	4642	5953
Independent reflections	3884	4642	3429
R_{int}	0.0629	0.0000	0.0288
Goodness-of-fit on F^2	1.037	1.123	1.132
R and *R*′ ($I > 2\sigma(I)$)	0.0987, 0.2451	0.0859, 0.2545	0.0532, 0.1402
(all data)	0.1645, 0.2811	0.1187, 0.2790	0.0793, 0.1533
Largest diff. peak and hole /eÅ^{-3}	0.648, −0.336	1.186, −0.806	0.650, −0.525

atoms had been located, it was obvious from the *Fourier* difference maps that solvent molecules were present in the asymmetric unit of these complexes. Thus, one toluene molecule, two H_2O molecules, and one CH_2Cl_2 molecule, disordered over two positions, were found for **1**, **2**, and **3**, respectively. The occupancy factors of two H_2O molecules were fixed to 0.50 and 0.25 in order to give reasonable isotropic thermal parameters and low *R* values. The same criteria led to an occupancy factor of 0.25 for two disordered positions of CH_2Cl_2 and 0.5 for toluene. The hydrogen atoms on the carbon atoms were included in calculated positions and given thermal parameters equivalent 1.2 times those of the atom to which they were attached. Hydrogen atoms of the H_2O molecules in **2** and CH_2Cl_2 in **3** were not introduced in the refinement process. In **1** and **2**, the PF_6^- anions were disordered. In both cases two sets of octahedral fluorine atoms were refined with occupancy factors of *x*, and $1 - x$, *x* being refined to 0.62(1) and 0.56(2) for **1** and **2**, respectively. The dimensions of CH_2Cl_2 in **3** as well as of PF_6^- in **1** and **2** were constrained during the refinement using the DFIX keyword. The toluene molecule was refined as a rigid body. In **1**, the metal centers as well as the phosphorus and oxygen atoms were refined with anisotropic thermal parameters, whereas the carbon atoms and chlorine atoms of CH_2Cl_2 were refined using only isotropic thermal parameters. The low quality of the X-ray data as indicated by the high final *R* values listed in Table 3 prevented the anisotropic refinement of all non-hydrogen atoms. The image plate pictures taken of the X-ray diffraction patterns from different crystals revealed a low degree of crystallinity. All non-hydrogen atoms of **2** and **3** were refined anistropically, except the disordered fluorine atoms, which were refined with isotropic group temperature factors in both complexes. The oxygen atoms of water molecules in **3** were also refined using isotropic thermal parameters. The structures were refined on F^2 until convergence using the

SHELXL program [15]. Molecular and crystal packing diagrams were drawn with the PLATON [16] and CERIUS2 [17] software. The X-ray date were deposited at the Cambridge Structural Data Base (**1**: CSD 147330; **2**: CSD 147331; **3**: CSD 147332).

Electrochemistry

The electrochemical instrumentation consisted of a BAS CV – 50 W Voltammetric Analyzer in connection with BAS/Windows data acquisition software. All electrochemical experiments were run under Ar at room temperature. Tetrabutylammonium hexafluorophosphate (Aldrich) was used as supporting electrolyte; it was recrystallized from ethanol. Cyclic voltammetry experiments were performed in a glass cell (MF-1082 from BAS) in a C-2 cell enclosed in a *Faraday* cage. The reference electrode was Ag/AgCl (MF-2079 from BAS, −44 mV relative to SCE). The reference eletrode was calibrated with a solution of ferrocene (1 m*M*) to obtain a potential in agreement with the literature value [18]. The auxiliary electrode was a 7.5 cm Pt wire (MW-1032 from BAS) with a gold-plated connector. The working electrode was a Pt disk (MF-2013 from BAS, ϕ *ca.* 0.022 cm^2) sealed in Kel-F plastic. Between each CV scan the wroking electrode was electrocleaned, polished on diamond and alumina, cleaned with H_2O/MeOH, and sonicated before use according to standard procedures as given in the equipment manual. Solvents were dried as described above.

DFT calculations

Density functional calculations [6] were carried out using the Amsterdam Density Functional (ADF) program [10] developed by *Baerends* and coworkers (release 2.3) [19]. The local exchange correlation potential of *Vosko*, *Wilk*, and *Nusair* was used [20] together with *Becke*'s nonlocal exchange [21] and *Perdew*'s correlation corrections [22]. Unrestricted calculations were performed for the paramagnetic complexes. The geometry optimization procedure was based on the method developed by *Versluis* and *Ziegler* [23] using non-local correction terms in the calculation of the gradients. Unrestricted calculations were performed for the cation.

The structure of **2** described above was used to prepare input files for full geometry optimization. The phenyl groups were replaced by hydrogen atoms. In all calculations a triple-ζ *Slater*-type orbital (STO) basis set was used for Cu and Fe (4s, 4p, 3d); triple-ζ STO augmented sets with a 3d single-ζ polarization function were used (C: 2s and 2p, Cl: 3s and 3p, P: 3s and 3p, H: 1s). A frozen core approximation was used to treat the core electrons of C (1s), P (1s, 2s, 2p), Cl (1s, 2s, 2p), and Cu and Fe (1s, 2s, 2p).

Acknowledgments

This work was supported by PRAXIS XXI under project PRAXIS/PCNA/C/QUI/103/96. We thank *Z. M. Tavares* for the elemental analysis (ITQB) and cyclic voltammetric experiments. *P. Pinto* thanks ITQB for a grant. *M. J. Calhorda*, *P. Pinto*, and *V. Félix* thank the TMR Transition Metal Clusters in Catalysis and Organic Synthesis. The University of Reading and EPSRC are thanked for funds for the Image Plate system.

References

[1] a) Pilloni G, Graziani R, Longato B, Corain B (1991) Inorg Chim Acta **190**: 165; b) Pilloni G, Corain B, Degano M, Longato B, Zanotti G (1993) J Chem Soc Dalton Trans 165; c) Pilloni G, Longato B (1993) Inorg Chim Acta **208**: 17; d) Pilloni G, Valle G, Corvaja C, Longato B, Corain B (1995) Inorg Chem **34**: 5910; e) Pilloni G, Longato B, Bandoli G, Corain B (1997) J Chem Soc Dalton Trans 819; f) Díez J, Gamasa MP, Gimeno J, Aguirre A, Garcia-Grande S (1999)

Organometallics **18**: 662; h) Pilloni G, Corain B, Degano M, Longato B, Zanotti G (1993) J Chem Soc Dalton Trans 1777; i) Pilloni G, Longato B, Corain B (1991) **420**: 57
[2] Fraústo da Silva JJR, Williams RJP (1991) The Biological Chemistry of the Elements. Clarendon Press, Oxford
[3] Allen FH, Davies JE, Galloy JJ, Johnson O, Kennard O, Mcrae CF, Watson DG (1991) J Chem Inf Comput Sci **31**: 204
[4] a) Lehn JM (1990) Angew Chem Int Ed Engl **29**: 1304; b) Braga D, Grepioni F (1994) Acc Chem Res **27**: 51; c) Calhorda MJ, Braga D, Grepioni F (1999) Transition Metal Clusters – The Relationship between Molecular and Crystal Structure, In: Braunstein P, Oro LA, Raithby PR (eds) Metal Clusters in Chemistry. Wiley-VCH, Weinheim; d) Braga D, Grepioni F, Orpen AG (eds) (1999) Crystal Engineering: from Molecules to Crystals, to Materials. Kluwer Academic Publishers, Dordrecht
[5] a) Pettinari C, Marchetti F, Cingolani A, Troyanov SI, Drozdov A (1998) J Chem Soc Dalton Trans 3335; b) Yam VW-W, Lee W-K, Lai T-F (1993) Chem Comm 1571; c) Yam VW-W, Lo KK-W, Cheung K-K (1996) Inorg Chem **35**: 3459; d) Díez J, Gamasa MP, Gimeno J, Aguirre A, Garcia-Grande S (1991) Organometallics **10**: 380; e) Yam VW-W, Fung WK-K, Cheung K-K (1998) Organometallics **17**: 3293; f) Yam VW-W, Lee W-K, Lai T-F (1993) Organometallics **12**: 2383; g) Díez J, Gamasa MP, Gimeno J, Lastra E, Aguirre A, Garcia-Grande S (1993) Organometallics **12**: 2213; h) Yam VW-W, Fung WK-K, Wong M-T (1997) Organometallics **16**: 1772; i) Díez J, Gamasa MP, Gimeno J, Aguirre A, Garcia-Grande S (1997) Organometallics **16**: 3684; j) Gamasa MP, Gimeno J, Lastra E, Solans X (1988) J Organomet Chem **346**: 277; k) Gamasa MP, Gimeno J, Lastra E, Aguirre A, Garcia-Grande S (1989) J Organomet Chem **378**: C11; l) Ford PC, Cariati E, Bourassa J (1999) Chem Rev **99**: 3625
[6] Parr RG, Yang W (1989) Density Functional Theory of Atoms and Molecules. Oxford University Press, New York
[7] Casellato U, Graziani R, Pilloni G (1993) J Crystallogr Spectrosc Res **23**: 571
[8] Neo SP, Zhou Z-Y, Mak TCW, Hor TSA (1994) J Chem Soc Dalton Trans 3451
[9] Calhorda MJ, Godinho MSSC, Mealli C (submitted)
[10] Amsterdam Density Functional (ADF) program, release 2.3 (1995) Vrije Universiteit Amsterdam, The Netherlands
[11] Kubas GJ (1990) Inorg Synth **28**: 68
[12] Woollins JD (1994) Inorganic Experiments. VCH, Weinheim
[13] Kabsch W (1988) J Appl Crystallogr **21**: 916
[14] Sheldrick GM (1983) Acta Crystallogr Sect A **39**: 158
[15] Sheldrick GM (1997) SHELX-97, University of Göttingen
[16] Spek AL (1999) PLATON, a Multipurpose Crystallographic Tool, Utrecht University, Utrecht, The Netherlands
[17] CERIUS 2, version 4.0 (1999) Molecular Simulations Inc., San Diego
[18] Nelson IV, Iwamoto RT (1963) Anal Chem **35**: 867
[19] a) Baerends EJ, Ellis D, Ros P (1973) Chem Phys **2**: 41; b) Baerends EJ, Ros P (1978) Int J Quantum Chem S**12**: 169; c) Boerrigter PM, teVelde G, Baerends EJ (1988) Int J Quantum Chem **33**: 87; d) teVelde G, Baerends EJ (1992) J Comp Phys **99**: 84
[20] Vosko SH, Wilk L, Nusair M (1980) Can J Phys **58**: 1200
[21] Becke AD (1987) J Chem Phys **88**: 1053
[22] a) Perdew JP (1986) Phys Rev B**33**: 8822; b) Perdew JP (1986) Phys Rev B**34**: 7406
[23] a) Versluis A, Ziegler T (1988) J Chem Phys **88**: 322; b) Fan L, Zeigler T (1991) J Chem Phys **95**: 7401

Received July 14, 2000. Accepted July 21, 2000